ELSEVIER

Catalysis Today 56 (2000) 379–387

CATALYSIS TODAY

www.elsevier.com/locate/cattod

Characterization by solid state ^{51}V NMR spectroscopy

A.A. Shubin (Ru-1), O.B. Lapina (Ru-1), D. Courcot (F-5) *

Laboratoire de Catalyse et Environnement, E.A. 2598, Université du Littoral-Côted'Opale, MREID, 145 Avenue Maurice Schumann, 59140 Dunkerque, France

Contributors: A.A. Shubin, O.B. Lapina (Ru-1); D. Courcot, A. Aboukaïs (F-5); B. Revel [1] ; M. Rigole, M. Guelton (F-6); S. Caldarelli, J.C. Vedrine (F-1)

Abstract

The fresh catalyst V_2O_5–WO_3/TiO_2 and catalyst used in SCR for 9000 h have been studied by the solid state ^{51}V NMR spectroscopy in static and MAS conditions. According to ^{51}V NMR in both samples the majority of vanadium sites are in a distorted octahedral environment similar to that in V_2O_5. There is a strong interaction between vanadium oxide and the support, but the concentration of vanadium atoms strongly bound to the surface is very small and can be detected only in MAS NMR experiments or after removing the excess of V_2O_5. There is no influence of WO_3 additives on the structure of the particles of V_2O_5, whereas the influence on the structure of strongly bounded V cannot be excluded. Combination of static (wide line) and MAS NMR techniques permit the characterization of not only the structure of the vanadium species but also small changes in their local environment. Hence these experiments show that there are some distortions of the local environment of vanadium sites of the vanadium oxide particles compared with the polycrystalline V_2O_5; treatment by SCR increases these distortions.

Keywords: Solid state ^{51}V NMR; Static and MAS experiments; SCR catalyst

1. Introduction

In recent years solid state high-resolution ^{51}V NMR has become a powerful tool for studying the local environment of nuclei in polycrystalline vanadium samples [1–11]. In general, three main types of interaction determine the lineshape of the polycrystalline NMR spectra of quadrupole nuclei: (i) the dipole interaction of the magnetic moment of the nucleus with the magnetic moments of other nuclei that broadens the NMR lines; (ii) the quadrupole interaction of the nucleus with the electric field gradient that splits the lines and contributes to the shift of the central transition; (iii) the chemical shielding interaction that changes the position of the lines and makes them asymmetric. In some cases, significant paramagnetic interaction could occur in catalysts, in relation to the redox properties of these *reactive* solids. In practice, the relation among these interactions determines the real lineshape of the spectra. Thus in a high magnetic field ($H_0 > 7T$), the lineshape of the central transition in ^{51}V NMR spectra is determined mainly by the anisotropy of the chemical shielding tensor. The conclusions on V coordination (tetrahedral or octahedral, regular or distorted) and the extent of association of vanadium oxygen polyhedra can be drawn based on the type and magnitude of the chemical shielding anisotropy.

New techniques which have appeared recently permit the precise extraction of all the parameters of chemical shielding and quadrupolar tensors (including relative orientation of tensors) that determined NMR

* Corresponding author. Tel.: +33-3-2865-8268; fax: +33-3-2865-8239.

0920-5861/00/$ – see front matter
PII: S0920-5861(99)00298-9

lineshape. Among these techniques are: SATRAS — the high speed magic angle spinning (MAS) with the precise analysis of the intensity of spinning sidebands (ssb) [12–16], high-resolution multiple quantum MAS NMR spectroscopy [17–20], especially designed spin-echo experiments [21,22], etc.

Herein we present the ^{51}V NMR characterization of the polycrystalline V_2O_5 and V_2O_5–WO_3/TiO_2 catalysts by both static and MAS NMR techniques.

2. Experimental

^{51}V NMR measurements have been made on Bruker MSL-400, DSX 400 and ASX 400 spectrometers ($\nu_0 = 105.2$ MHz for ^{51}V resonance) using spin-echo and one-pulse (wide line and MAS) techniques. MAS spectra of powders were recorded at rotation frequencies of 6–15 kHz using 4 and 5 mm (outer diameter) rotors and the NMR probes from Bruker and constructed by Jakobsen [23]. Repetition time of 0.1–2 s and the rf pulse angle of about $\pi/12$ (corresponding to rf pulse duration of 2 and 1 μs for Bruker High Power and MAS probes, respectively) were used in the experiments. The NMR spectra distortions resulting from the finite rf excitation and NMR probe *Q*-factor were minimized by recording the spectra with different frequency offsets and applying subsequent numerical correction which is necessary for quantitative analysis of SATRAS experimental data [14]. All chemical shieldings are referenced to $VOCl_3$ as an external standard. For better phasing and minimizing of baseline distortions in NMR spectra, the linear prediction (backward LP-SVD method) of the first few (2–6) free induction decay (FID) data points and, in evident cases, polynomial baseline corrections were used.

Simulations of ^{51}V static and MAS NMR spectra were performed taking into account the second-order quadrupole correction (although it was not necessary in this case) and using the general purposes NMR1 program described earlier [24]. A particular variant of this program especially adopted to the fast computation of ssb intensities in MAS experiments (Herzfeld and Berger approach [25]) was used for SATRAS simulations and least-squares fittings. Computations were performed on an IBM PC compatible computer with P-90 processor and a SUN Sparc Station 10 equipped with 90 MHz ROSS Hyper Sparc CPUs.

Samples were first studied *as received*. The influence of the outgassing procedure was evaluated after a vacuum treatment performed at 300°C for 12 h. A procedure to remove the excess of V_2O_5 was attempted using diluted nitric acid solution at ambient temperature. Samples were then completely washed with distilled water, dried and calcined at 300°C.

3. Results and discussion

3.1. Static ^{51}V NMR spectra

It is a well known fact that the so-called instrumental effects (such as “dead time”, the bandwidth of the probe, phasing effects) influence the ^{51}V NMR lineshape of solid samples [6,14]. Nevertheless, for powdered samples (the case typically met in heterogeneous catalysis) it is common that only the central transition ($-1/2 \leftrightarrow +1/2$) can most probably be observed, while other transitions are too broad to be detected. This permits the use of single pulse excitation as a preliminary step of the investigation (taking into account that these spectra represent only a small fraction of the actual signal from V^{5+} sites). In the case of high-field ^{51}V NMR, the lineshape of the central transition is mainly determined by the chemical shielding anisotropy. The type and the magnitude of the chemical shielding anisotropy can serve as a reliable criteria for characterization of V coordination and the extent of association of vanadium–oxygen polyhedra.

Fig. 1 shows ^{51}V static wide line NMR spectra of V_2O_5 (Fig. 1a) and both fresh and used V_2O_5–WO_3/TiO_2 catalysts without any additional treatment (Fig. 1b and c). The spectra were recorded with the use of single pulse excitation at 105.25 MHz and linear prediction of the first two FID points.

It is clearly seen that the spectra of the fresh and used catalysts and V_2O_5 exhibit similar shape and position so that these spectra can be typically ascribed to the V^{5+} sites in a distorted octahedral environment. It is also evident that for this particular case, at least for pure V_2O_5 and fresh catalysts, not only central transition, but also satellite transitions are observable in the one-pulse spectra. Some changes of the line-

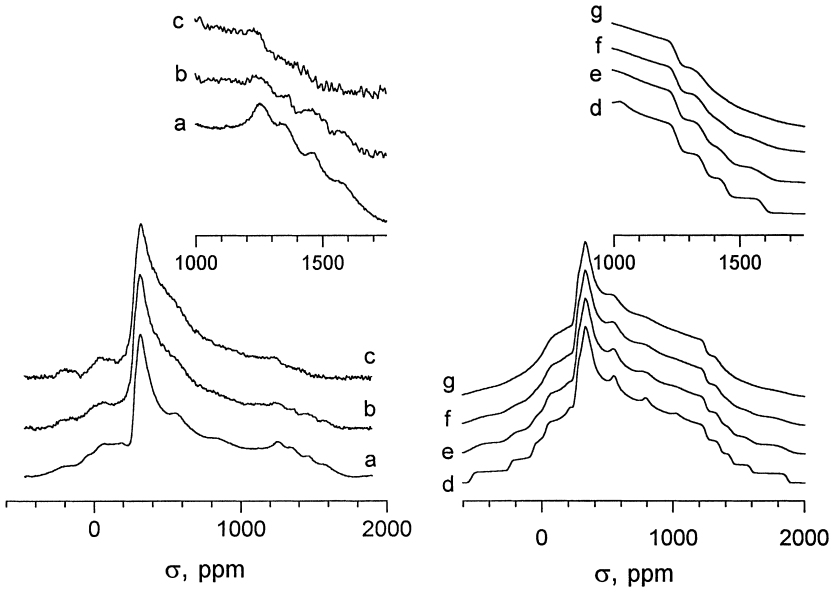

Fig. 1. Wide line one-pulse 105.25 MHz ^{51}V NMR spectra. (a) V_2O_5, (b) fresh V_2O_5–WO_3/TiO_2 catalyst without vacuum outgassing, (c) used V_2O_5–WO_3/TiO_2 catalyst without vacuum outgassing. Simulated one-pulse spectra (data set 5 from Table 1) with quadrupolar constant C_Q distributed around 799 kHz in a Gaussian-like fashion $g(x) = \left(1/\Delta_Q\sqrt{2\pi}\right)\exp(-x^2/2\Delta_Q^2)$, (d) $\Delta_Q = 0$, (e) $\Delta_Q = 50$ kHz, (f) $\Delta_Q = 75$ kHz, (g) $\Delta_Q = 100$ kHz.

shape observed for catalyst samples in comparison with polycrystalline V_2O_5 (broadening and smashed of the characteristic points) can be explained by the following reasons: (i) distribution of NMR parameters due to the imperfect structure of V_2O_5 dispersed over the TiO_2 surface; (ii) increase of the individual NMR line width due to the presence of paramagnetic species; (iii) superposition of several lines.

The standard vacuum outgassing procedure results in partial catalyst reduction that diminishes the intensity of NMR signal due to the presence of paramagnetic V^{4+} species. The intensity of the ^{51}V NMR signal after standard vacuum outgassing diminishes about four times for both fresh and used catalysts (Fig. 2, spectra b,e). NMR signals from ^{51}V nuclei located near V^{4+} are unobservable or are significantly broadened as may be seen from the spectra. Water adsorption is accompanied by the formation of $[H_2VO_4]^-$ species (narrow signal with $\delta = -559$ ppm in Fig. 2c and f) that indicate the pH ~ 7 of the water condensed on the catalyst surface [26].

Since ^{51}V is a quadrupole nucleus additional NMR experiments (high speed MAS experiments) allowed us to obtain parameters characterizing chemical shielding and quadrupole interaction for pure V_2O_5. After comparison with the results known from the literature these parameters were used as the starting point for the interpretation of ^{51}V NMR spectra of the catalysts under study.

3.2. Magic angle spinning spectra

High speed MAS NMR with the subsequent analysis of the intensities of all spinning sidebands (SATRAS technique) was used for V_2O_5 in order to extract additional information about chemical shielding and quadrupolar tensors along with their relative orientation. Fig. 3 shows the spinning sideband pattern obtained for V_2O_5 and for both fresh and used catalysts with the rotation speed of 6–8 kHz. All these spectra are characterized by only one set of spinning sidebands and the same value of isotropic shift $\sigma_{iso} = -612$ ppm. Nevertheless, the intensities of the sidebands, as well as the envelope of MAS spinning sidebands, and a wide line in the bottom of the spec-

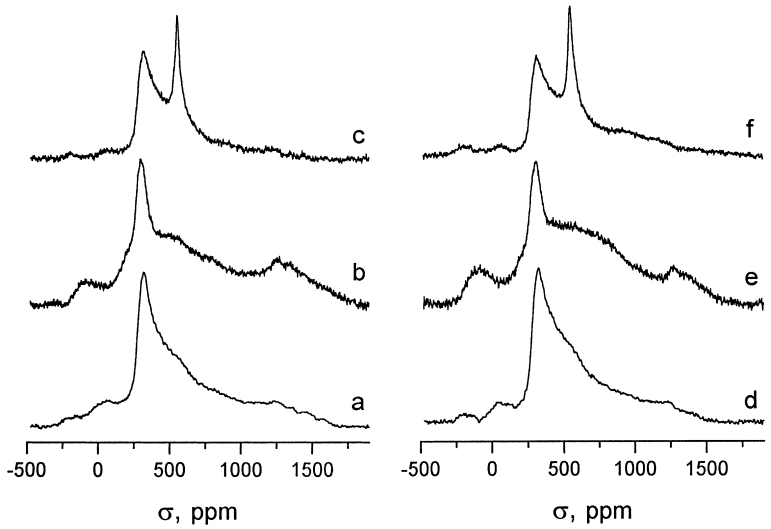

Fig. 2. Static ^{51}V NMR spectra of V_2O_5–WO_3/TiO_2 catalysts at 105.25 MHz recorded using single pulse excitation. (a)–(c): Fresh catalyst; (d)–(f): used catalyst. (a) and (d): spectra measured without vacuum outgassing; (b) and (e): spectra of the vacuum outgassed catalysts; (c) and (f): after water adsorption on the catalysts.

tra are quite different for all samples. To clarify the changes revealed in the spectra some simulations of MAS NMR spectra were performed.

Analysis of the intensities of the spinning sidebands for pure V_2O_5 with the least-squares fitting of seven parameters started from the values of interaction parameters chosen near the literature values [12,15], results in two local minimums for both $\nu_r = 5.860$ and $\nu_r = 6.836$ kHz (Table 1). It is obvious that data sets 1 and 3 from Table 1 correspond to the same minimum, moreover, the root-mean-square deviations for them are about 1.5 times smaller then for data sets 2 and 4, accordingly. An average between data sets 1 and 3 (data set 5 in Table 1) parameters was chosen for V_2O_5 and used in subsequent spectra simulations. Note that these parameters are slightly different from previous values, mainly the large value of the asymmetry parameter $\eta_Q = 0.21$ for quadrupole coupling. Nevertheless, they reproduce with a high quality the MAS spectrum of V_2O_5. Fig. 4 demonstrates experimental MAS ^{51}V NMR spectrum of V_2O_5 along with the experimental and numerically fitted ssb intensities. The broad line in the bottom of the MAS NMR spectra of the catalysts (Fig. 3b and c) may come, in principle, from two different sources. It may be the influence of the distribution of interaction parameters

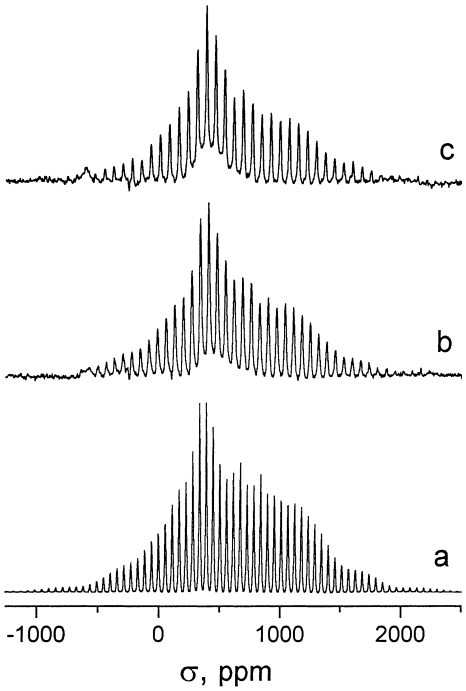

Fig. 3. 105.25 MHz ^{51}V MAS NMR spectra. (a) V_2O_5 at spinning frequency $\nu_r = 5.86$ kHz, (b) V_2O_5–WO_3/TiO_2 fresh catalyst at $\nu_r = 7.375$ kHz, (c) V_2O_5–WO_3/TiO_2 used catalyst at $\nu_r = 7.98$ kHz.

Table 1
^{51}V quadrupole tensor parameters (C_Q, η_Q)[a], chemical shielding tensor parameters (δ_σ, η_σ, σ_{iso})[b], and Euler angles (α, β, γ) describing the relative orientation of quadrupole tensor with respect to chemical shielding tensor for V_2O_5 from 105.25 MHz ^{51}V MAS NMR

Data set	ν_r (kHz)	No. of ssb's[c]	C_Q (kHz)	η_Q	δ_σ (ppm)	η_σ	σ_{iso}	α (deg)[d]	β (deg)	γ (deg)[d]
1	5.860	74	799	0.22	635	0.09	612[e]	146	127	139
2	5.860	74	811	0.04	625	0.09	–	141	127	5
3	6.836	59	799	0.20	637	0.13	–	133	128	151
4	6.836	59	813	0.18	635	0.13	–	126	128	31
5			799	0.21	636	0.11	–	140	127.5	145
(Mean data from 1 to 3)										

[a] Nuclear electric quadrupole moment eQ, electric field gradient tensor eigenvalues (V_{xx}, V_{yy}, and $V_{zz} = eq$) are connected with C_Q and η_Q by the relations: $C_Q = e^2qQ/h$; $V_{xx} = 1/2(-1-\eta_Q)V_{zz}$; $V_{yy} = 1/2(-1+\eta_Q)V_{zz}$.

[b] The eigenvalues of chemical shielding tensor are expressed by δ_σ, η_σ and σ_{iso} in the following manner: $\sigma_{xx} = 1/2\delta_\sigma(-1-\eta\sigma)+\sigma_{iso}$; $\sigma_{yy} = 1/2\delta_\sigma(-1+\eta_\sigma)+\sigma_{iso}$; $\sigma_{zz} = \delta_\sigma + \sigma_{iso}$.

[c] Number of spinning sideband intensities used in optimization.

[d] Angles α and γ are determined with significant error because the symmetry of chemical shielding tensor and quadrupole tensor is close to axial.

[e] σ_{iso} was determined from the position of zero spinning sideband and presented here without second-order quadrupole shift correction which is about 0.1 ppm in this case and is significantly smaller then the error connected with the use of external standard $VOCl_3$ (its concentration, temperature, etc.).

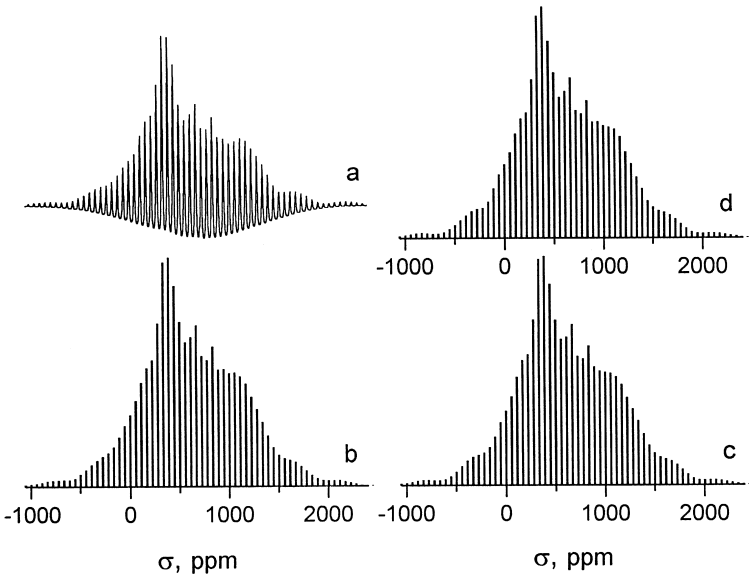

Fig. 4. (a) Experimental ^{51}V MAS NMR spectrum of V_2O_5 at $\nu_r = 5.86$ kHz (the same as Fig. 3a, but shown without baseline correction), (b) stick plot of integrated experimental ssb intensities for V_2O_5. (c) and (d) simulated ssb intensities at the same ν_r, (c) with data set 5 from Table 1, (d) with data set 2 from Table 1.

around the values typical for V_2O_5 or another (one or more) broad signal overlapping with V_2O_5-like spectrum. The ^{51}V MAS spectra dependence on the Gaussian-like distribution of the quadrupolar constant C_Q around the value for V_2O_5 is demonstrated in Fig. 5. The difference in the envelope of MAS spinning sidebands for Fig. 5a and d is detectable but nevertheless small. At the same time, the difference caused by C_Q distribution is more observable in the one-pulse spectra of static samples. Simulated static spectra (Fig. 1d–g) may be directly compared with the experimental (Fig. 1a–c). The visual comparison of these

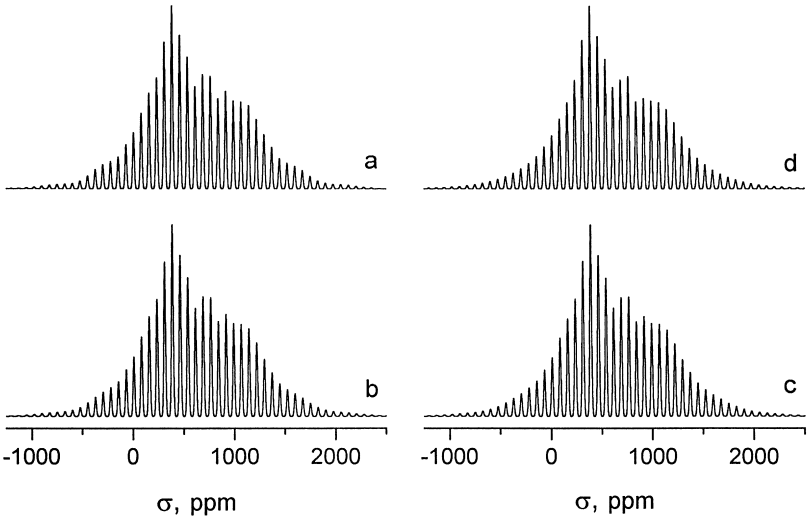

Fig. 5. Simulated 105.25 MHz ^{51}V MAS NMR spectra of V_2O_5 at $\nu_r = 7.98$ kHz using data set 5 from Table 1 and quadrupolar constant C_Q distributed around 799 kHz in a Gaussian-like fashion. (a) $\Delta_Q = 0$, (b) $\Delta_Q = 50$ kHz, (c) $\Delta_Q = 100$ kHz, (d) $\Delta_Q = 200$ kHz. Individual NMR line width was Gaussian with $\Delta = 0.9$ kHz.

spectra shows that the V_2O_5-like signal in the fresh catalyst may be characterized by the effective distribution of the quadrupolar constant with the distribution $\Delta_Q = 50$–75 kHz, while for the used catalyst $\Delta_Q \approx 100$ kHz or larger for the V_2O_5-like part NMR signal. Simulated MAS spectra with distributed C_Q (Fig. 5) do not show any broad line in the base of the spectra. It may be expected only for significantly large (few MHz) quadrupole constants and quadrupole parameters distribution widths, when the second-order quadrupole effects are noticeable. For this case more sophisticated models of parameters distribution exist

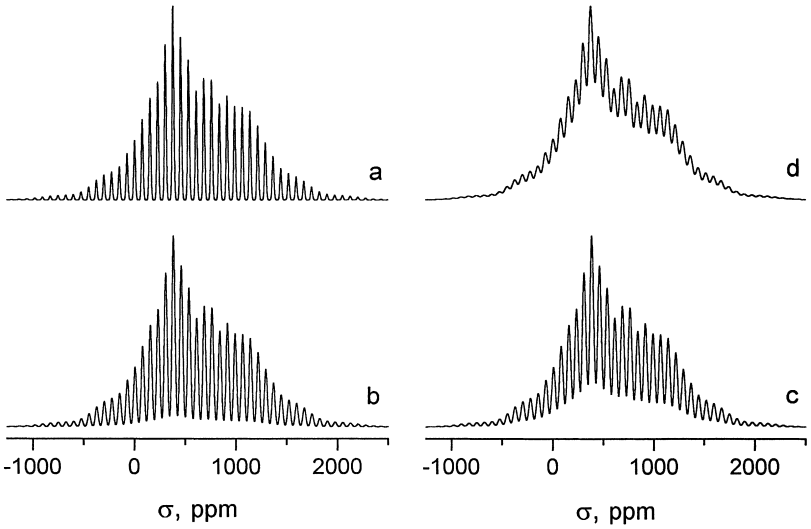

Fig. 6. Simulated 105.25 MHz ^{51}V MAS NMR spectra of V_2O_5 at $\nu_r = 7.98$ kHz using data set 5 from Table 1 and σ_{yy} distributed around its initial value in a Gaussian-like fashion. (a) $\Delta_\sigma = 0$, (b) $\Delta_\sigma = 35$ ppm, (c) $\Delta_\sigma = 50$ ppm, (d) $\Delta_\sigma = 75$ ppm. Individual NMR line width was Gaussian with $\Delta = 0.9$ kHz.

[14]. Simulated MAS spectra with any principal component of chemical shielding tensor or σ_{iso} distributed around V_2O_5 values (Fig. 6 is the typical example) demonstrate the possibility of obtaining broad lines in the bottom of the spectra (Fig. 6c and d). Nevertheless, we have to exclude this reason (at least, for Gaussian-like parameters distribution) because experimentally observed (Fig. 3b and c) line widths of all spinning sidebands (even for sidebands with the large numbers on the spectra edges) are smaller than ssb line widths in Fig. 6c and d (which are necessary to reproduce the broad line in the spectra). Therefore, the broad line in the ^{51}V NMR spectra of catalysts should be assigned to another signal with parameters significantly different from those for V_2O_5. More detailed information may be obtained from 15 kHz rotation speed ^{51}V MAS NMR experiments when spinning sidebands of very minor species seem to be observable (Fig. 7a). In this case for the fresh catalyst one signal is detected in addition to that of V_2O_5. The unshifted band with the variation of spinning speed was found at $\sigma_{iso} = -664$ ppm (species 2). Unfortunately due to the significant overlapping of spinning sidebands from the V_2O_5-like signal and this new one it is difficult to determine the exact values of all magnetic resonance parameters. It is obvious from the spectrum that only the signal with $\sigma_{iso} = -664$ ppm is characterized by a significantly larger chemical shielding anisotropy. MAS NMR spectra of the used catalyst recorded at 15 kHz (Fig. 7b) show the presence of V_2O_5 like species and the species with $\sigma_{iso} = -664$ ppm but with less intensity in comparison with the fresh catalyst. In addition, a third species (species 3) seems to be revealed at these rotation speeds. From its $\sigma_{iso} = -553$ ppm value and the envelope of sidebands pattern, this signal is consistent with a polymeric surface vanadium species in a distorted environment and has already been observed in the case of unpromoted V_2O_5/TiO_2 catalysts [11]. To complete the observation of the minor signal (broad line and/or species 2 and 3) with spinning rates of 6–15 kHz, measurements at very high rotation have been performed at 35 kHz, using a new Bruker probe. The main conclusions are (Fig. 8):

1. A real difference exists between the fresh catalyst spectrum (Fig. 8b) and V_2O_5 spectrum (Fig. 8a). This difference can be attributed to the broad line previously observed (6–15 kHz). Nevertheless, at 35 kHz rotation, this broad line appears narrower, which suggests that these species probably originate from very strong interactions with the support.
2. With 35 kHz rotation, we cannot say whether or not species 2 at −664 ppm previously observed with 15 kHz rotation is present, due to overlapping with the broad signal. Then, information concerning species 2 (and consequently species for the used catalyst) must be considered with some care.

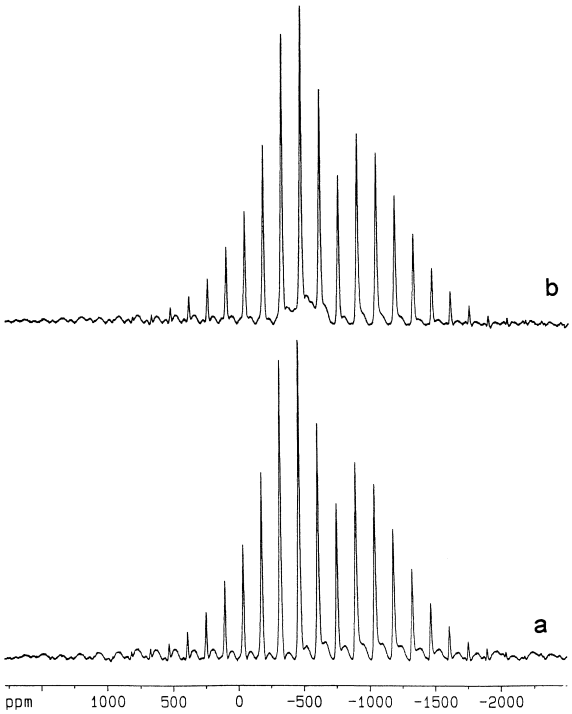

Fig. 7. ^{51}V MAS NMR spectra of fresh (a) and used (b) samples recorded at 105.2 MHz at spinning frequency ν_r of 15 kHz.

In addition, at the present stage of knowledge it is difficult to attribute signal 2 with $\sigma_{iso} = -664$ ppm in fresh and used catalysts to any influence of WO_3 promoter on V^{5+} chemical shielding. Nevertheless, comparison with literature data [4,7,11,27,28] shows that in binary V_2O_5/TiO_2 systems no such signal has been observed yet. The presence of signal 2 could arise from other constituent compounds in the solid: SiO_2, Al_2O_3, CaO, or SO_4^{2-}.

Thus, the following conclusions on the structure of the catalysts can be drawn from the MAS data:

(i) MAS NMR spectra of fresh and used catalysts indicated that the significant part of V^{5+} ions

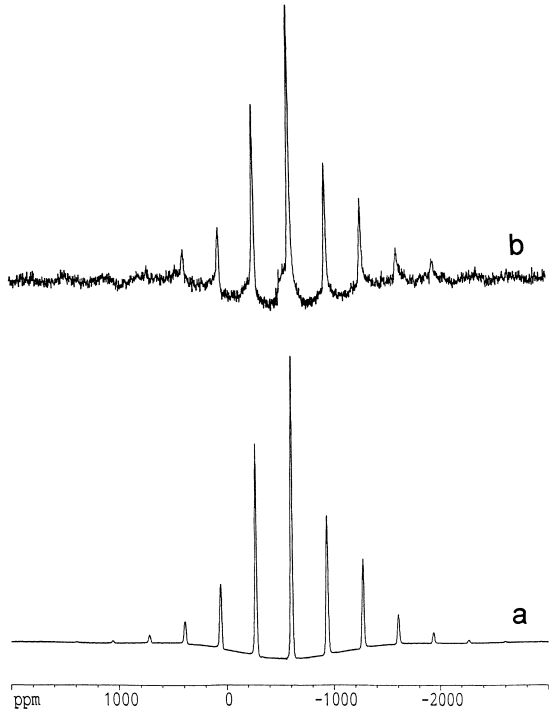

Fig. 8. ^{51}V MAS NMR spectra of pure V_2O_5 (a) and fresh sample (b) recorded at 105.2 MHz at spinning frequency ν_r of 35 kHz.

occupied one type of V sites close to that in V_2O_5; (ii) there is some distribution of NMR quadrupolar parameters (for the V_2O_5-like part of the spectra) in the catalysts compared with polycrystalline V_2O_5; (iii) the catalyst treatment increases defects in the structure (which follows from the increase in the distribution of NMR parameters and the more intensive broad signal in the used catalyst); (iv) there are probably two other types of vanadium sites in V_2O_5–WO_3/TiO_2, one of which (signal 3) may be attributed to vanadium strongly bounded with the TiO_2 support and another one (signal 2) may be caused by the presence of elements different from TiO_2 which are components of the solid, but their content is very low.

3.3. Static and MAS spectra of the vanadia strongly bounded to titania

The removal of the excess of V_2O_5 from the catalysts surface results in the spectra presented in Fig. 9. It is clearly seen that the spectra of vanadium strongly bounded with the titania surface differ markedly from V_2O_5 and from each other. Spectra of the strongly bounded vanadia correspond to more distorted vanadium environments, moreover these spectra could be the superposition of different lines from inequivalent vanadium sites. It is not possible to compare these spectra with the analogs for the catalysts V_2O_5/TiO_2 without WO_3 additive. Therefore, we could not make any conclusion about the influence of WO_3 on the structure. At the same time, conclusions about the influence of the treatment procedure on the structure of the strongly bound vanadia could be made easily.

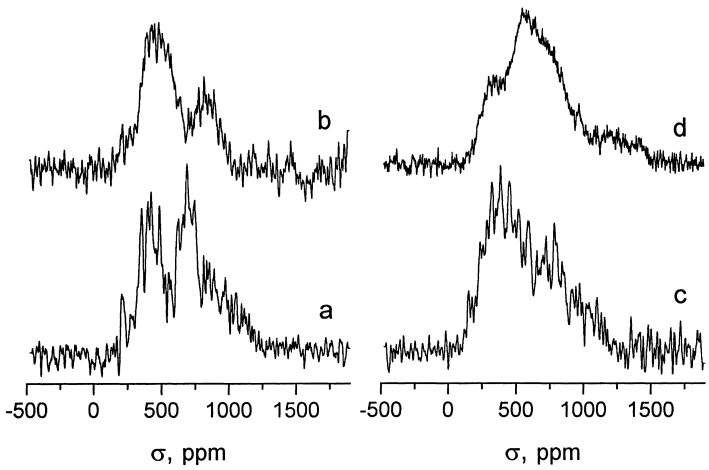

Fig. 9. 105.25 MHz one-pulse static and $\nu_r = 6.4$ kHz MAS ^{51}V NMR spectra of washed V_2O_5–WO_3/TiO_2 catalyst. (a), (b): Fresh catalyst; (c), (d): used catalyst. (a), (c): MAS spectra; (b), (d): static spectra.

4. Conclusions

Comparison of the data obtained for V_2O_5–WO_3/TiO_2 catalysts with the ^{51}V NMR results for VO_x/TiO_2 catalysts presented in literature [3–8,11] permits us to make the following conclusions.

Most of the vanadium (V) atoms detected in V_2O_5–WO_3/TiO_2 catalysts are in a distorted octahedral environment and are most likely in a similar structure to V_2O_5. Surface isolated and monolayer species that could be observed in catalysts prepared by grafting or other procedures [8] are not detected in this case. Nevertheless, some peculiarities of the observed structure should be emphasized.

1. There is a strong interaction between V_2O_5 and the support, but the concentration of vanadium atoms strongly bounded to the surface is very small. This strongly bounded vanadium may be detected in high speed MAS NMR experiments or after removing excess V_2O_5.
2. The local environment of vanadium sites of the V_2O_5 particles in the catalysts are more distorted as compared with the polycrystalline V_2O_5; treatment under reaction conditions increases the distortion.
3. There is no influence of paramagnetic V^{4+} on the structure of V^{5+} in the "towers" of V_2O_5.
4. There is no influence of WO_3 additives on the structure of the "towers" of V_2O_5, whereas the influence on the structure of strongly bound V could be supposed.

Acknowledgements

The authors thank V.V. Terskikh, B. Mouchel and Dr. A.V. Nosov for help with NMR experiments and useful discussion. We are indebted to Professor J.P. Amoureux, Professor C. Fernandez and Bruker for the use of 35 kHz MAS facilities. The Region Nord-Pas de Calais is gratefully acknowledged for the financial support for purchasing the ASX 400 spectrometer, and the Russian Foundation for Basic Research for partial support (grant RFBR N 98-03-32323a) for the work.

References

[1] B. Taouk, M. Guelton, J. Grimblot, J.P. Bonnelle, J. Phys. Chem. 92 (1988) 6700.
[2] O.B. Lapina, A.V. Simakov, V.M. Mastikhin, S.A. Veniaminov, A.A. Shubin, J. Mol. Catal. 50 (1989) 55.
[3] H. Eckert, I.E. Wachs, J. Phys. Chem. 93 (1989) 6796.
[4] H. Eckert, G. Deo, I.E. Wachs, A.M. Hirt, Colloids Surfaces 45 (1990) 347.
[5] G. Deo, A.M. Turek, I.E. Wachs, T. Machej, J. Haber, N. Das, H. Eckert, A.M. Hirt, Appl. Catal. 91 (1992) 27.
[6] O.B. Lapina, V.M. Mastikhin, A.A. Shubin, V.V. Krasilnikov, K.I. Zamaraev, Prog. NMR spectrosc. 24 (1992) 457.
[7] C. Fernandez, M. Guelton, Ph. Bodart, M. Rigole, F. Lefebvre, Catal. Today 20 (1994) 77.
[8] L.G. Pinaeva, O.B. Lapina, V.M. Mastikhin, A.V. Nosov, B.S. Balzhinimaev, J. Mol. Catal. 88 (1994) 311.
[9] R.H.H. Smits, K. Seshan, J.R.H. Ross, A.P.M. Kentgens, J. Phys. Chem. 99 (1995) 9169.
[10] V.M. Mastikhin, O.B. Lapina, Vanadium catalysts: solid state NMR, NMR Encyclopedia 8 (1996) 10771.
[11] D. Courcot, B. Grzybowska, Y. Barbaux, M. Rigole, A. Ponchel, M. Guelton, J. Chem. Soc. Faraday Trans. 92 (1996) 1607.
[12] J. Skibsted, N.C. Nielsen, H. Bildsoe, H.J. Jakobsen, Chem. Phys. Lett. 188 (1992) 405.
[13] J. Skibsted, N.C. Nielsen, H. Bildsoe, H.J. Jakobsen, J. Am. Chem. Soc. 115 (1993) 7351.
[14] C. Jager, NMR Basic Principles and Progress 31 (1994) 133.
[15] C. Fernandez, P. Bodart, J.P. Amoureux, Solid State NMR 3 (1994) 79.
[16] J. Skibsted, T. Vosegaard, H. Bildsoe, H. Jakobsen, J. Am. Chem. Soc. 100 (1996) 14872.
[17] J.P. Amoureux, C. Fernandez, L. Carpentier, E. Cochon, Phys. Stat. Sol. (a) 132 (1992) 461.
[18] L. Frydman, J.S. Harwood, J. Am. Chem. Soc. 117 (1995) 5367.
[19] J.-P. Amoureux, C. Fernandez, L. Frydman, Chem. Phys. Lett. 259 (1996) 347.
[20] S.P. Brown, S.J. Heyes, S. Wimperis, J. Magn. Reson. Ser. A 119 (1996) 280.
[21] J. Haase, E. Oldfield, J. Magn. Reson. Ser. A 101 (1993) 30.
[22] P.P. Man, Phys. Rev. B 52 (1995) 9418.
[23] H.J. Jakobsen, P. Daugaard, V. Langer, J. Magn. Reson. 76 (1988) 162.
[24] A.A. Shubin, O.B. Lapina, G.M. Zhidomirov, Abstracts, IXth AMPERE Summer School, Novosibirsk, USSR, 20–26 September 1987, p. 103.
[25] J. Herzfeld, A.E. Berger, J. Chem. Phys. 73 (1980) 6021.
[26] E. Heath, O.W. Howarth, J. Chem. Soc. Dalton (1981) 1105.
[27] D. Courcot, P. Bodart, C. Fernandez, M. Rigole, M. Guelton, J. Chim. Phys. 91 (1994) 909.
[28] G. Deo, I.E. Wachs, J. Phys. Chem. 95 (1991) 5889.